

Drosophila Fragile X-Related Gene Regulates the MAP1B Homolog Futsch to Control Synaptic Structure and Function

Yong Q. Zhang,^{1,4} Adina M. Bailey,^{2,4}
Heinrich J.G. Matthies,¹ Robert B. Renden,¹
Mark A. Smith,¹ Sean D. Speese,¹ Gerald M. Rubin,²
and Kendal Broadie^{1,3}

¹Department of Biology

University of Utah

Salt Lake City, Utah 84112

²Howard Hughes Medical Institute

Department of Molecular and Cell Biology

University of California, Berkeley

Berkeley, California 94720

Summary

Fragile X mental retardation gene (*FMR1*) encodes an RNA binding protein that acts as a negative translational regulator. We have developed a *Drosophila* fragile X syndrome model using loss-of-function mutants and overexpression of the *FMR1* homolog (*dfxr*). *dfxr* nulls display enlarged synaptic terminals, whereas neuronal overexpression results in fewer and larger synaptic boutons. Synaptic structural defects are accompanied by altered neurotransmission, with synapse type-specific regulation in central and peripheral synapses. These phenotypes mimic those observed in mutants of microtubule-associated Futsch. Immunoprecipitation of dFXR shows association with *futsch* mRNA, and Western analyses demonstrate that dFXR inversely regulates Futsch expression. *dfxr futsch* double mutants restore normal synaptic structure and function. We propose that dFXR acts as a translational repressor of Futsch to regulate microtubule-dependent synaptic growth and function.

Introduction

Fragile X syndrome (FraX) is the most common inherited disease causing mental retardation. The defect was identified as a trinucleotide CGG expansion in the regulatory region of *fragile X mental retardation 1* (*FMR1*), causing transcriptional silencing and loss of the gene product, FMRP (Verkerk et al., 1991; Verheij et al., 1993). FMRP is widely expressed in fetal and adult tissues, with pronounced expression in brain and testis where major symptoms are manifested (Devys et al., 1993). FMRP is predominantly in the cytoplasm with occasional nuclear staining (Devys et al., 1993; Verheij et al., 1993). FMRP contains nuclear localization (NLS) and export (NES) signals (Eberhart et al., 1996), suggesting that it functions as a nucleo-cytoplasmic shuttle protein. FMRP contains three RNA binding domains: two K homology (KH) domains and one RGG box (Ashley et al., 1993a; Siomi et al., 1993). FMRP binds ~4% of human fetal brain mRNA in vitro, but the targets are largely unknown, except its own mRNA and myelin basic pro-

tein mRNA (Ashley et al., 1993a; Brown et al., 1998). FMRP associates with polyribosomes (Khandjian et al., 1996; Tamanini et al., 1996; Feng et al., 1997a) and functions as a negative translational regulator (Laggerbauer et al., 2001; Li et al., 2001; Schaeffer et al., 2001).

FraX neurological pathogenesis has attracted intensive analysis. Cerebral cortical autopsies from FraX patients show abnormal neuronal dendritic spine morphology, postulated to be associated with synaptic immaturity (Hinton et al., 1991; Irwin et al., 2001). In *FMR1* knockout mice, longer and denser dendritic spines are observed, consistent with the human phenotype (Comery et al., 1997; Nimchinsky et al., 2001). FMRP is observed at synapses in the developing rat brain (Weiler et al., 1997) and is present in mouse brain synaptosomes (Feng et al., 1997b; Tamanini et al., 1997). Furthermore, FMRP mRNA associates with translational complexes in synaptic subcellular fractions, and the expression of FMRP is increased within minutes of glutamate receptor stimulation, suggesting that FMRP acts as a synaptic activity-dependent translational regulator (Weiler et al., 1997; Jin and Warren, 2000). These different lines of evidence suggest that the underlying mechanism of mental retardation in FraX patients is the result of defective synapse development or function.

We have generated a *Drosophila* FraX model to specifically address the hypothesis that FMRP regulates synaptic development and function. Wan et al. (2000) identified the *Drosophila* homolog of *FMR1*. We mutated *Drosophila* dFXR (*Drosophila* fragile X related) and assayed its roles in synaptic development and function in two model systems in *Drosophila*: the eye and the neuromuscular junction (NMJ). We show that the level of dFXR protein regulates both synaptic structure and function. The *dfxr* synaptic phenotypes mimic defects observed in mutants with altered levels of Futsch, a microtubule-associated protein with homology to mammalian MAP1B (Hummel et al., 2000; Roos et al., 2000). We further demonstrate that dFXR associates with *futsch* mRNA and negatively regulates Futsch expression. Most importantly, we show that a *dfxr futsch* double mutant restores the *dfxr* synaptic structural and functional defects in the eye and NMJ. Our results suggest that dFXR is acting as a translational repressor of Futsch to regulate the synaptic microtubule cytoskeleton and that Futsch misregulation is sufficient to explain both synaptic structure and function defects characterizing the *Drosophila* FraX model.

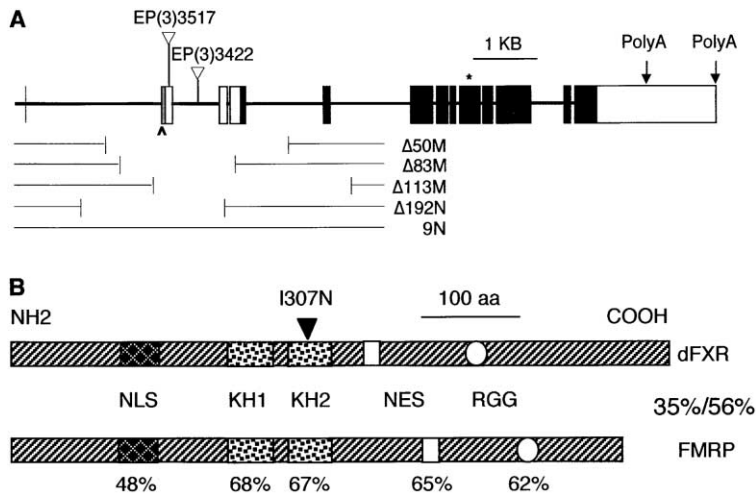
Results

Molecular Characterization of *Drosophila fragile X related* (*dfxr*) Gene

In a systematic gain-of-function screen for genes involved in eye development, a P element insertion line EP(3)3517 under sev-GAL4 control produced a mild rough eye phenotype (Rorth et al., 1998). The flanking genomic sequence of EP(3)3517 matched a group of overlapping EST (expressed sequence tag) clones with

³Correspondence: broadie@biology.utah.edu

⁴These authors contributed equally to this work.



FMRP, with the percent amino acid identity between the homologs indicated. The point mutation I307N used in overexpression studies is indicated. Abbreviations are as follows: KH, K homology domain; NLS, nuclear localization signal; NES, nuclear export signal; and RGG, a motif rich in arginine and glycine.

high homology to human *FMR1*. Two representative EST clones were fully sequenced. To reveal the gene structure, we determined the genomic sequence of *dfxr* from P1 clone DS05441. Intron-exon organization of *dfxr* inferred from comparison of the genomic sequence and the cDNA sequences is depicted in Figure 1A. No CGG repeat was found in the 422 bp 5' UTR (untranslated region) of *dfxr*, while a CGG repeat was found within 200 bp 5' UTR of *FMR1* (Ashley et al., 1993b). Whole *Drosophila* genome sequence search showed no other significantly homologous genes. dFXR appears to be a prototype of the FMRP family that evolved to give rise to the three members of the mammalian family (FMRP, FXR1P, and FXR2P). Sequence comparison using CLUSTAL W shows that the dFXR (AF205596) has 35% and 56% overall identity and similarity, respectively, to FMRP, 37% and 65% to FXR1P, and 36% and 65% to FXR2P. The N-terminal 383 amino acids (aa) of dFXR have a higher homology (50%/84%) than the C-terminal 298 aa to the corresponding segments of FMRP. Similar to FMRP, dFXR contains three RNA binding domains: two KH domains and one RGG box, a NLS and a NES (Figure 1B; Wan et al., 2000).

Extensive alternative splicing produces different isoforms of human FMRP (Ashley et al., 1993b). Comparison of multiple *dfxr* EST sequences and genomic sequence demonstrated that alternative splicing occurs across the gene. 5' UTR alternative splicing and 3' alternative polyadenylation were found (Figure 1A). The 1 kb difference of the two major bands detected in Northern blots (Wan et al., 2000) is consistent with the differential 3' polyadenylation. Alternative splicing in the coding region resulting in three extra amino acids in the second KH2 domain was also noted (Figure 1A). So far, the functional significance of this alternative splicing is unclear.

To study the functions of dFXR via a genetic approach, we first mapped the gene via polytene chromosome in situ hybridization to 85F9-12 on the third chromosome. The original insertion EP(3)3517 maps in the 5' UTR of the *dfxr* gene, and another insertion EP(3)3422 maps in the second intron of *dfxr* gene (Figure 1A). Subsequent

Figure 1. Molecular Characterization of *dfxr* Gene and Mutants

(A) Genomic structure of *dfxr* and mapping of mutants. Intron-exon organization of *dfxr* is shown at the top. The insertion sites of two P element lines EP(3)3517 and EP(3)3422 at the 5' region of *dfxr* are indicated. Introns are indicated by solid horizontal lines, exons by vertical lines or boxes, and coding regions by black boxes. The shaded box underlined by a carat (^) in the second exon is alternatively spliced out in a variant transcript. The asterisk indicates an alternative splicing site in the coding region. Two alternative polyA sites are indicated by vertical arrows. Shown below are four deletions ($\Delta 50M$, $\Delta 83M$, $\Delta 113M$, and $\Delta 192N$) with breakpoints indicated and a revertant (9N) derived from imprecise and precise excision of EP(3)3517, respectively. The scale bar shows 1 kb.

(B) Protein domains in dFXR and human

remobilization of EP(3)3517 produced four deletions of *dfxr* (Figure 1A). All four deletions were characterized by DNA sequencing, and their breakpoints are presented in Figure 1A. Anti-dFXR staining of these different alleles showed that the two EP insertion lines are hypomorphs (data not shown), whereas the four *dfxr* specific deletions appear to be protein nulls, since no dFXR staining was detected by immunostaining (Figure 2B).

dFXR Protein Is Cytoplasmic and Highly Enriched in Nervous System

A specific monoclonal dFXR antibody has been characterized by Western and immunoprecipitation analyses (Wan et al., 2000). We genetically confirmed the antibody specificity (Figure 2B) and performed a systematic expression study of the protein throughout the fly life cycle (Figure 2). dFXR expression was first widely detected in many tissues in stage 5 embryos. In late stage 16 embryos, strong dFXR expression was present in brain lobes, ventral nerve cord (VNC), and muscles (data not shown; Wan et al., 2000). In the third instar larva, most (or perhaps all) of the neurons in the VNC and brain expressed high levels of dFXR (Figure 2A). Double-labeling with dFXR antibody and propidium iodide, a dye used to visualize nuclei, showed that dFXR was abundant in soma cytoplasm as well as in neuronal processes within the CNS and peripheral nerves exiting the CNS (Figure 2C). In addition to the CNS expression, high levels of dFXR were also observed in larval imaginal discs, testis, and ring gland (data not shown). In adult brain, dFXR was also expressed in most (or perhaps all) of the neurons and highly enriched in optic lobes and distinct clusters of cells within the central brain (Figure 2D). The conspicuous dFXR expression in the central complex is interesting, as this structure regulates coordinated motor control (Ilius et al., 1994) and alterations of dFXR expression in flies led to locomotory defects (see below).

dFXR was observed in the cytoplasm, rather than the nucleus, of all the cells examined including all neurons and muscles (Figures 2A-2E). Even after dFXR overex-

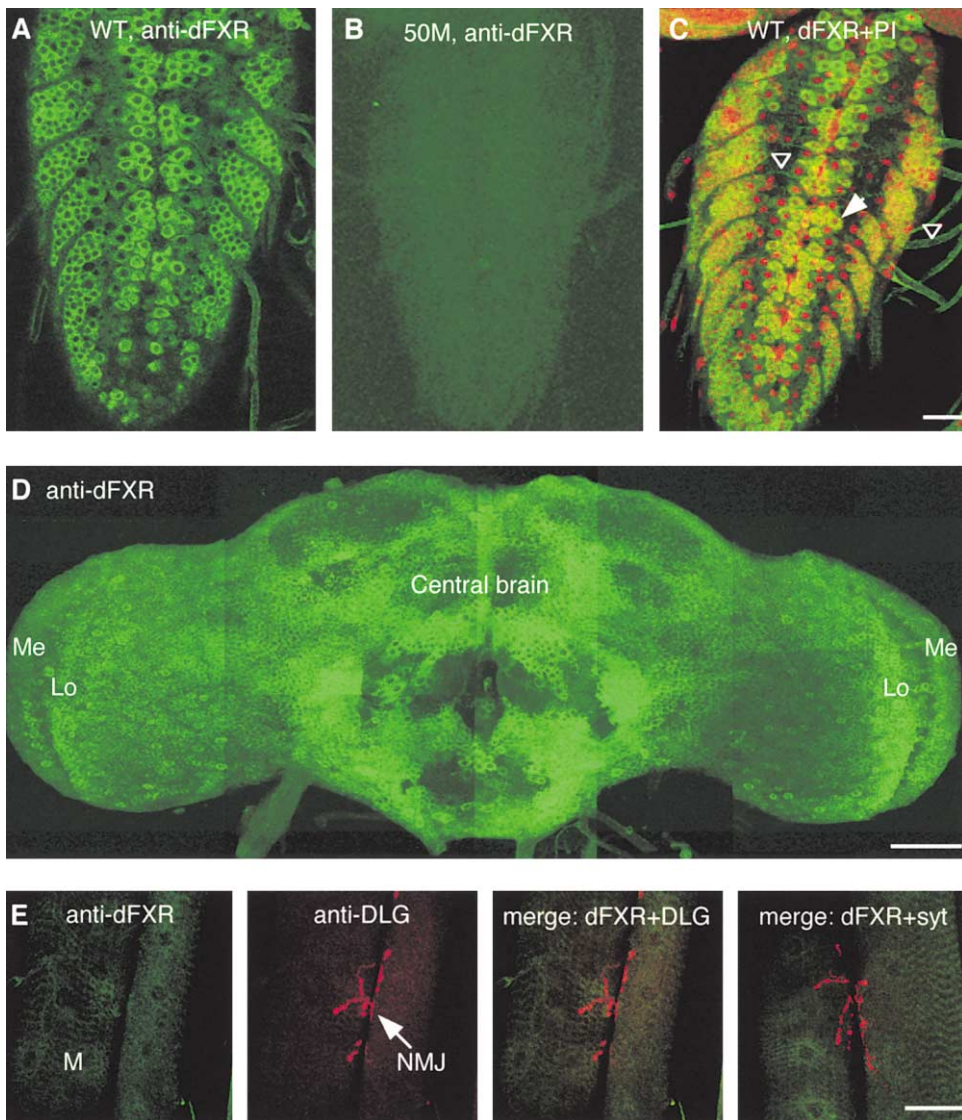


Figure 2. dFXR Is Cytoplasmic and Highly Expressed in the Nervous System

(A) dFXR protein is cytoplasmic and highly expressed in all neurons along the midline and lateral sides of the third instar ventral ganglion. (B) No dFXR-specific staining was detected in a *dfxr* deletion line 50M. (C) dFXR is present in neuronal cell bodies (arrow) and axonal processes (open arrowheads) throughout the nervous system. Double-staining of a third instar ventral ganglion was done with dFXR antibody (in green) and propidium iodide (in red) to visualize nuclei. The scale bar equals 10 μm for (A)–(C). (D) dFXR is highly expressed in adult brain. A projection of serial confocal sections of the whole brain is shown. dFXR is enriched in optic lobes (Me indicates medulla and Lo indicates lobula) and neuronal clusters in the central brain. The scale bar equals 50 μm . (E) dFXR is expressed at a lower level in muscles and is not specifically enriched at the NMJ. At left is an image stained with anti-dFXR (M indicates muscle), and second from left is an image stained with postsynaptic anti-DLG. Middle right is a merged image of dFXR and DLG antibody staining. At right is a merged image double-stained with anti-dFXR (green) and presynaptic anti-syt (red). The scale bar equals 20 μm .

pression as described below, only cytoplasmic staining was observed (data not shown). These observations are consistent with the subcellular localization of mammalian FMRP, although occasional nuclear localization has been observed (Devys et al., 1993; Verheij et al., 1993). Mammalian FMRP has also been localized at synapses by immunoelectron microscopy (Weiler et al., 1997) and synaptosomal preparation analyses (Feng et al., 1997b; Tamanini et al., 1997). We therefore performed double-labeling experiments with dFXR antibody and synaptic marker antibodies, e.g., synaptotagmin (syt) and Discs

Large (DLG). We observed that dFXR was not enriched at central synapses in the VNC neuropil (Figures 2A and 2C) nor in peripheral NMJ synapses (Figure 2E). Thus, dFXR is highly expressed in neurons, moderately expressed in muscles, is globally cytoplasmic, but it is not enriched in synapses.

Overexpression and Mutation of dFXR Produce Neuromuscular Defects

Since dFXR is an RNA binding protein (Wan et al., 2000), it might be predicted that dFXR overexpression would

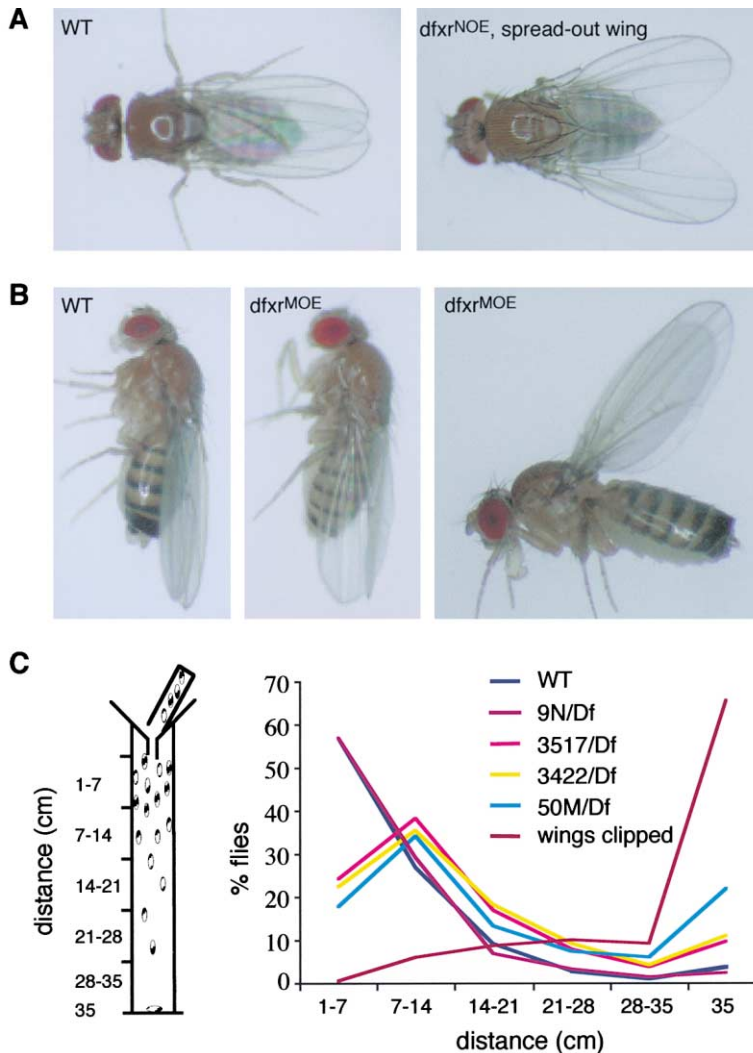


Figure 3. *dfxr* Overexpression Lines and Nulls Display Postural and Locomotive Defects as Viable Adults

(A) *dfxr^{NOE}* gave rise to distinctive postural defects. At left is dorsal wild-type (wt) wing posture; at right, spread-out wing in *dfxr^{NOE}* mutants.

(B) *dfxr^{MOE}* gave rise to different wing posture phenotypes. At left is lateral wild-type (wt) wing posture, in the middle, droopy wings, and at right, held-up wings when dFXR is overexpressed in muscles.

(C) *dfxr* null mutants have compromised flight ability. At left is a schematic diagram of the apparatus for flight test (see Experimental Procedures). At right is the flight performance of different genotypes. The x axis represents the vertical positions (in cm) where the flies landed in the cylinder, and the y axis represents the percentage of flies. The genotypes are color coded. Wild-type and the revertant 9N/Df perform identically and fly well. Three dFXR alleles over deficiency (Df) show similarly impaired flight. The label “wings clipped” represents the positive control of no flight ability. At least 130 flies were tested for each genotype.

titrate out its RNA substrates. Therefore, we overexpressed dFXR in numerous tissues using the UAS-GAL4 transgenic system (Brand and Perrimon, 1993). Two *dfxr* UAS constructs, UAS-dFXR and UAS-I307N (the same point mutation as the human I304N in the second KH RNA binding domain; Jin and Warren, 2000), were transformed into the fly genome.

When either dFXR construct was driven by panneuronal elav-GAL4, the progeny exhibited abnormally spread-out wings and could not fly (Figure 3A, *dfxr^{NOE}*). These animals were uncoordinated and displayed early adult lethality, usually 5–10 days following adult eclosion. When either dFXR construct was driven by *mhc*-GAL4, which drives overexpression in all muscles, the progeny showed droopy or held-up wings and could not fly (Figure 3B, *dfxr^{MOE}*). When either dFXR construct were driven by G7-GAL4, which drives higher muscle expression, all progeny died at pupal stages (data not shown). These results suggest that dFXR expression level is critical for normal neuromusculature functions. It is interesting to note that overexpression of human FMRP in the mouse model also produced behavioral abnormalities (Peier et al., 2000).

The overexpression of I307N by GAL4 lines in wild-type background consistently produced similar but weaker phenotypes than did the overexpression of wild-type dFXR (Figures 4A and 4B). To examine the functional significance of the mutation I307N, we compared phenotypes caused by cooverexpression of wild-type and I307N dFXR with that caused by overexpression of each alone. Cooverexpression of both in the nervous system caused lethality with few escapers, whereas overexpression of either wild-type or I307N alone produced viable adults with eye/wing phenotypes. These results suggest that the point mutation I307N is not a dominant negative, but rather acts as a simple hypomorph, supporting previous conclusions (Wan et al., 2000).

All six *dfxr* mutant alleles, including four deletion nulls (Figure 1A), are viable with no discernible morphological phenotypes. A range of behavioral tests including bang sensitivity, temperature sensitivity, and phototaxis assays did not show detectable differences between wild-type and null mutants. However, the mutants showed defective coordinated behavior in a simple flight test (Figure 3C). The two EP insertion lines, EP(3)3517 and EP(3)3422, and a *dfxr* null (50M), each over deficiency

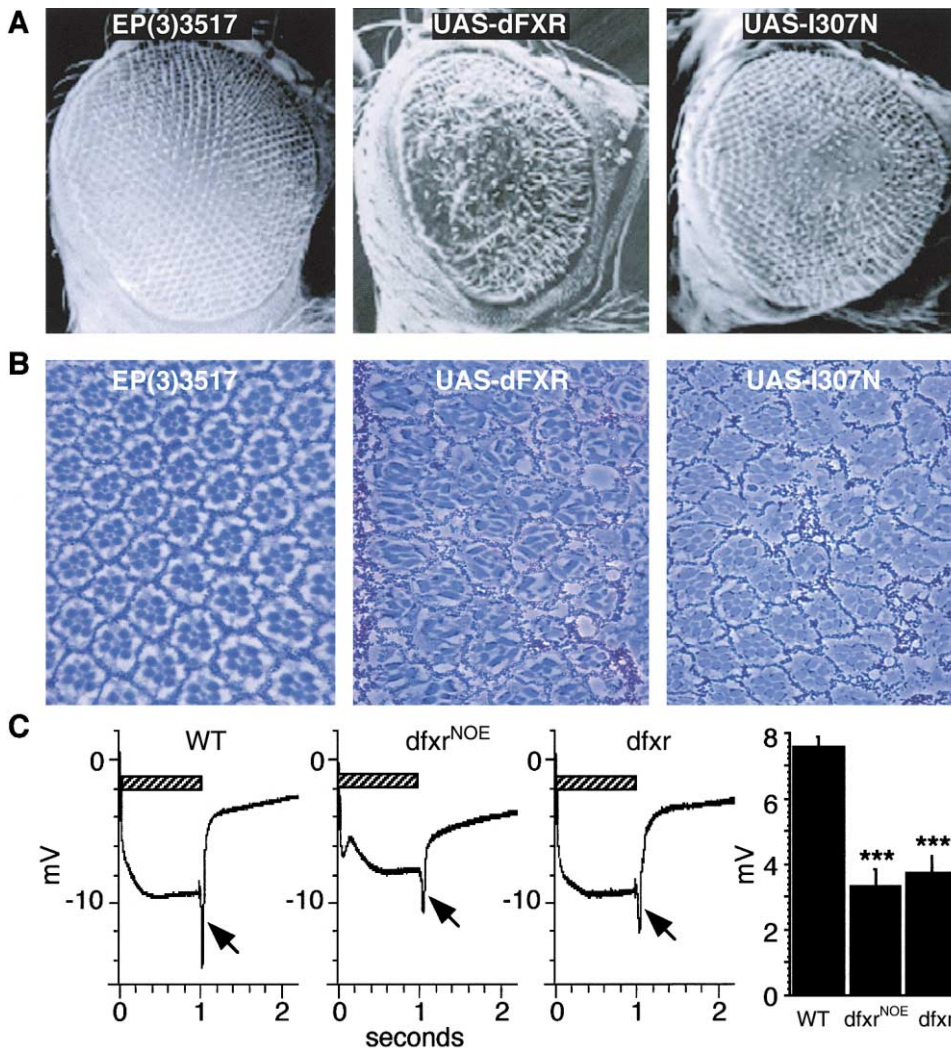


Figure 4. Overexpression and Loss-of-Function of dFXR Gave Rise to Structural and Functional Eye Phenotypes

(A) dFXR overexpression by sev-GAL4 resulted in rough eyes. Overexpression of the original EP(3)3517 produced a mild rough eye phenotype. Overexpression of I307N generated a similar but milder phenotype than that of wild-type dFXR.

(B) dFXR overexpression by sev-GAL4 resulted in an abnormal photoreceptor pattern in tangential sections. Overexpression of EP(3)3517 had a near wild-type pattern. Again, the mutant I307N phenotype was similar but less severe than wild-type.

(C) Both *dfxr* nulls and *dfxr*^{NOE} lines had decreased synaptic transmission measured via electroretinograms (ERGs). At left, ERG traces from wild-type (wt), *dfxr*^{NOE} mutants, and nulls (*dfxr*). Hatched bars indicate the duration of the light stimulus. The arrows point to the “off-transient” photoreceptor synaptic current. At right, both *dfxr* NOE and nulls had a similar ~50% impairment of synaptic transient amplitude (mV). The three asterisks indicate $p < 0.001$ by Student’s *t* test ($n \geq 5$). Error bars are SEM.

Df(3R)by62, were flight defective (Figure 3C). The flight defect was specific to the *dfxr* mutations, since the phenotype was rescued by precise excision of the EP insertion (Figure 3C, 9N). Flight tests on single animals confirmed the flight defect of *dfxr* mutants (data not shown). Flies with neuronal or muscle overexpression of dFXR are also flight defective, most likely due to their wing postural defects (Figures 3A and 3B).

dFXR Regulates Photoreceptor Structure and Neurotransmission

One of the best-established systems to study neuronal structure and function in *Drosophila* is the adult eye. To assay the effect of dFXR on retinal neuronal patterning, we first overexpressed the protein by using UAS-dFXR

constructs and eye-specific GAL4 drivers. UAS-dFXR driven by sev-GAL4 produced significant retinal disorder (Figures 4A and 4B). The disorder included misshapen rhabdomeres, abnormal numbers of rhabdomeres per ommatidium, and fused ommatidia (Figure 4B). The UAS-I307N lines produced phenotypes similar but milder than wild-type UAS-dFXR (Figures 4A and 4B), demonstrating a specific role of the KH2 RNA binding domain in these phenotypes, consistent with Wan et al. (2000). In contrast, *dfxr* null mutants produced no detectable effect on the structure of the eye (data not shown). Thus, overexpression of dFXR can specifically perturb neuronal patterning in the eye, but the protein is not required for the process.

Electroretinogram (ERG) assays were performed on

different *dfxr* genotypes to assay phototransduction and synaptic transmission between photoreceptors and laminar interneurons. Both neuronal overexpression of dFXR driven by *elav-GAL4* (*dfxr^{NOE}*) and null mutants (*dfxr*) displayed a robust photoreceptor response, as indicated by depolarization of the photoreceptor throughout the 1 s light pulse (Figure 4C). The plateau potential was similar to the controls (Figure 4C), even when the photoreceptor morphology is disrupted (similar to that shown in Figures 4A and 4B). Thus, neither *dfxr* null mutation nor *dfxr^{NOE}* perturbs phototransduction.

Depolarization of photoreceptors triggers release of the neurotransmitter histamine, which targets inhibitory Cl^- channels in the postsynaptic cell. The synaptic response commonly referred to as the “off-transient” in ERGs (arrows in Figure 4C) is caused by the closure of the histaminergic Cl^- channels and resulting depolarization of the laminar cell (Broadie, 2000). Off-transients were measured as the magnitude of negative potential change at termination of the light pulse. Both *dfxr^{NOE}* and *dfxr* null mutants showed similar significant decreases in the characteristic response of the postsynaptic laminar cell to cessation of photoreceptor depolarization (Figure 4C). Compared to control, *dfxr^{NOE}* showed a 56% decrease and *dfxr* null showed a 51% decrease in off-transient mean amplitude (Figure 4C, right). Thus, changes in the level of dFXR, both increase and decrease, strongly impair synaptic transmission in the visual system.

dFXR Regulates Synaptic Structure at the NMJ

The second well-defined system for studying synaptic structure and neurotransmission in *Drosophila* is the larval neuromuscular junction (NMJ). Importantly, the glutamatergic NMJ is amenable to detailed single-cell assays of pre- and postsynaptic mechanisms. We have shown that dFXR is expressed both in presynaptic motor neurons and in postsynaptic muscles during embryonic development and in larvae (Figure 2). We therefore analyzed *dfxr* nulls and transgenic lines with dFXR overexpressed either pre- and postsynaptically. Since the cellular phenotype associated with human *FraX* patients and *FMR1* knockout mice is alterations in synaptic morphology (Hinton et al., 1991; Comery et al., 1997; Irwin et al., 2001; Nimchinsky et al., 2001), we first determined if synaptic structural defects were present in *Drosophila*.

Significant alterations in NMJ synaptic terminals were observed in *dfxr* mutants. First, *dfxr* null mutants displayed pronounced synaptic overgrowth and overelaboration of synaptic terminals (Figure 5A, *dfxr*). This phenotype is reminiscent of the dendritic spine overgrowth observed in mammalian mutants. Quantification of the number of synaptic boutons on muscle 4 revealed that the *dfxr* nulls had a 51% increase over controls (Figure 5C, left). Second, *dfxr^{NOE}* caused the opposite phenotype of synaptic undergrowth (Figure 5A) and displayed an average 36% decrease in the number of muscle 4 synaptic boutons (Figure 5C, left). Postsynaptic dFXR MOE caused a similar but a more modest loss of structural elaboration and exhibited a 17% decrease in muscle 4 synaptic boutons (Figure 5A,C). Quantification of the muscle 6/7 NMJ boutons showed a similar trend (Figure 5C). In addition to the increased bouton number, *dfxr* null mutants showed excessive arboreal branching

(Figure 5A). The muscle 4 NMJ contained ~50% more synaptic branches than control (Figure 5C). In contrast, dFXR overexpression had no significant impact on synaptic branching (Figure 5C). Thus, the level of dFXR on both sides of the synaptic cleft is an important determinant of synaptic growth.

dFXR also plays a role in regulating bouton morphology. Overexpression of dFXR presynaptically caused an obvious enlargement of single synaptic boutons (Figure 5B, *dfxr^{NOE}*). The NMJ bouton diameter in *dfxr^{NOE}* animals was nearly twice that of wild-type (Figure 5C, right). Increased bouton size was not limited to type 1b boutons; type 1s boutons were also larger (Figure 5B; for bouton types, see Beumer et al., 1999). This phenotype is specific to presynaptic overexpression, since null mutants and postsynaptic overexpression showed bouton size comparable to control (data not shown). In summary, *dfxr* null mutants showed synaptic overelaboration with increased synaptic branching and bouton differentiation, whereas overexpression caused the opposite undergrowth phenotype with fewer synaptic boutons which, in the case of *dfxr^{NOE}* mutants, were structurally enlarged.

dFXR Regulates Neurotransmission at the NMJ

We next assayed synaptic transmission at the NMJ. Unlike the eye, the glutamatergic NMJ is amenable to detailed, single-cell recordings of synaptic function using two electrode voltage clamp techniques, which can be used to dissect pre- and postsynaptic transmission mechanisms. We therefore asked whether the NMJ in *dfxr* mutants displayed altered communication, due to changes in either presynaptic glutamate release or postsynaptic glutamate response.

Significant alterations in NMJ neurotransmission were observed in *dfxr* mutants. First, evoked synaptic transmission was significantly elevated in *dfxr* null mutants (Figure 6A, *dfxr*). The mean excitatory junctional current (EJC) amplitude was increased from 35 nA in controls to 66 nA in *dfxr* null mutants. The variance of transmission amplitude (SD/mean current amplitude), a measure of synaptic fidelity, was unaffected in *dfxr* compared to wild-type, demonstrating that the average synaptic efficacy was upregulated in null mutants. dFXR NOE in the presynaptic terminal did not significantly alter mean EJC amplitude (Figure 6A). Second, quantal analyses of miniature excitatory junctional currents (mEJCs) showed that the frequency of spontaneous glutamate release was increased by 5-fold in *dfxr^{NOE}* animals (Figure 6B) but was not changed with postsynaptic *dfxr^{MOE}* (Figure 6B). mEJC frequency in *dfxr* null mutants was mildly increased relative to controls (Figure 6B, *dfxr*). There was no striking increase in mEJC amplitude in any of the *dfxr* genotypes (Figure 6C). We conclude that dFXR modulates synaptic transmission through a primarily presynaptic mechanism. Loss of dFXR results in elevated evoked neurotransmission, whereas presynaptic overexpression results in elevated spontaneous vesicle fusion.

To summarize, we have shown that *dfxr* mutants perturb synaptic neurotransmission at two different synapse types: histaminergic photoreceptor (central) synapses and glutamatergic NMJ (peripheral) synapses. Surprisingly, increase and decrease of dFXR levels similarly alters

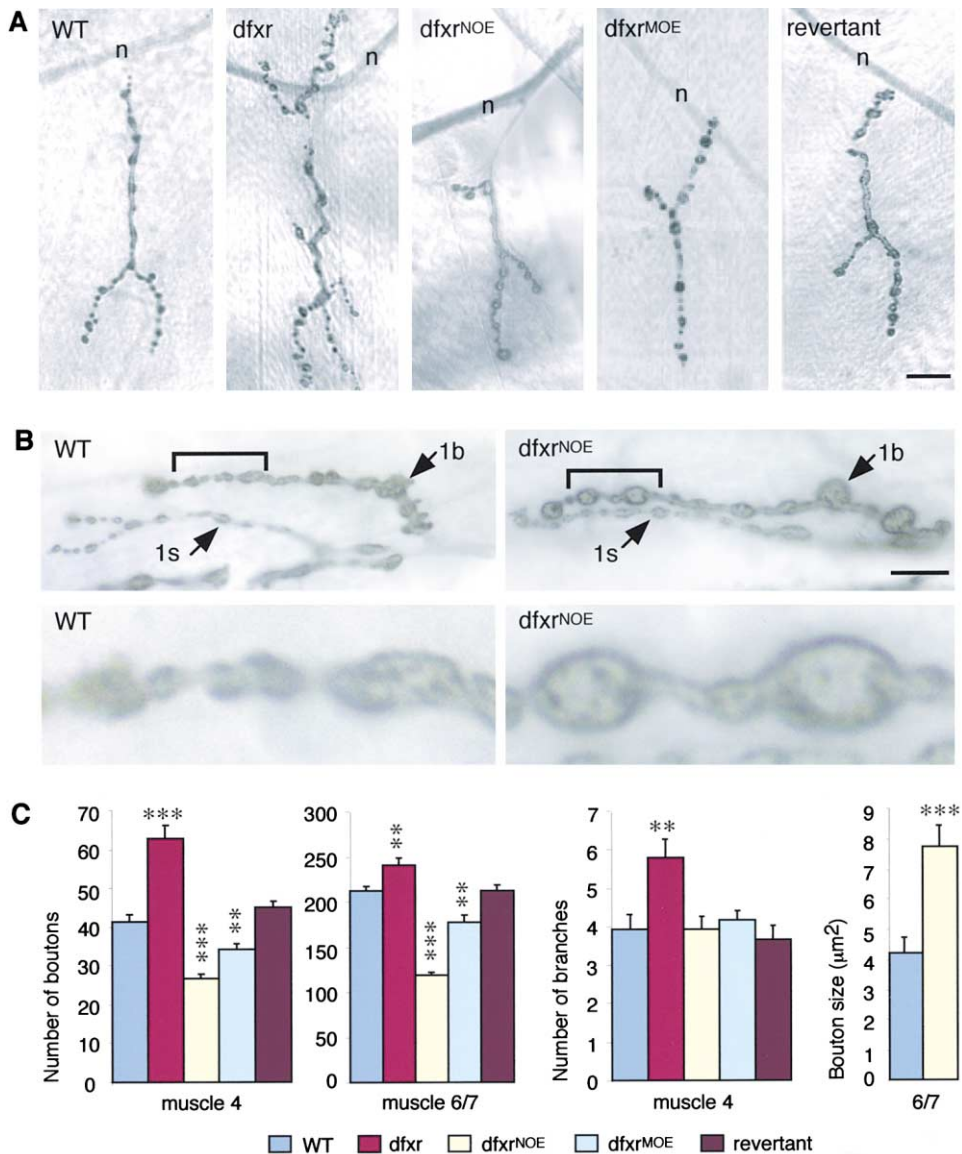


Figure 5. *dfxr* Mutants and Overexpression Lines Differentially Affect Synaptic Growth and Structure

(A) Images show third instar muscle 4 NMJ type 1b terminals labeled with synaptic marker anti-CSP. *dfxr* nulls (*dfxr*) display overgrown synaptic terminals. Both dFXR NOE and MOE caused undergrown terminals. Precise excision line 9N displays wild-type NMJ structure (revertant). “n” indicates segmental nerve innervating muscle 4. The scale bar equals 10 μm.

(B) dFXR NOE specifically lead to enlarged synaptic boutons. Parts of NMJ terminal for muscle 6 were shown for wt and NOE mutants. Type 1b and 1s boutons are indicated by arrows. The lower two images show type 1b synaptic boutons at higher magnification. The scale bar equals 10 μm.

(C) Quantification of synaptic structural phenotypes. At left, the numbers of synaptic boutons quantified for muscle 4 and muscle 6/7 NMJs are shown. For all genotypes, n ≥ 20. In the middle, the numbers of type 1b synaptic branches on muscle 4 are shown; n ≥ 20. At right, the synaptic bouton area (μm²) is shown. At least 100 type 1b boutons from muscle 6/7 were quantified for each genotype. Statistical significance was calculated using Mann-Whitney U test (two asterisks indicate p < 0.01; three asterisks indicate p < 0.001). Error bars indicate SEM.

presynaptic function in these two synapse types, suppressing transmission in central synapses and elevating it in peripheral synapses. The fact that the polarity of the regulation differs could be attributed to a multitude of differences between the two synaptic classes.

The *Drosophila* MAP1B Homolog Futsch Is Negatively Regulated by dFXR

FMRP has recently been shown to be a negative translational regulator (Laggerbauer et al., 2001; Li et al., 2001;

Schaeffer et al., 2001). What potential targets for dFXR could explain its regulation of synaptic structure and transmission in the eye and NMJ? Futsch, the *Drosophila* homolog of the mammalian microtubule-associated protein MAP1B, regulates the microtubule cytoskeleton to mediate dendritic, axonal, and synaptic growth (Hummel et al., 2000; Roos et al., 2000). Hypomorphic *futsch* mutants have recently been shown to display a distinctive NMJ morphology phenotype similar to *dfxr*^{NOE}, i.e., fewer and larger synaptic boutons (Roos et al., 2000).

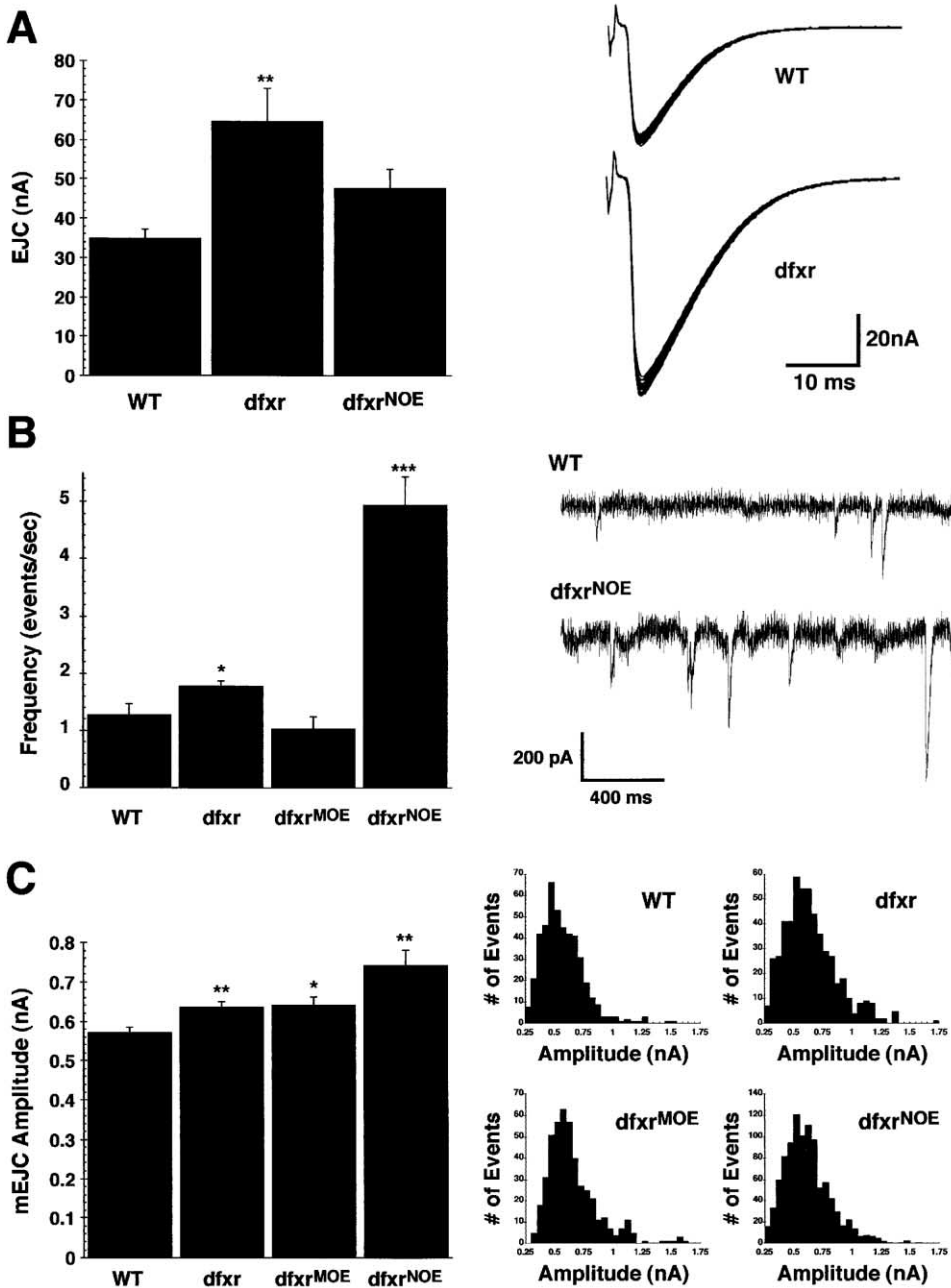


Figure 6. *dfxr* Nulls and Overexpression Lines Differently Affect Evoked and Spontaneous Neurotransmission

(A) Neurally evoked excitatory junctional currents (EJCs) were significantly increased in *dfxr* nulls (*dfxr*) compared to control (wt). At left, mean EJC amplitudes are shown; two asterisks indicate $p < 0.01$ by Student's *t* test. Error bars are SEM; $n \geq 10$ for all genotypes. At right, sample EJC traces from controls and *dfxr* nulls.

(B) Miniature EJC (mEJC) frequency is increased 5-fold in dFXR NOE mutants and slightly increased in nulls (*dfxr*). At left, mean mEJC frequency. One asterisk indicates $p < 0.05$, and three asterisks indicate $p < 0.001$ by Mann-Whitney U test; $n \geq 8$ for all genotypes. Error bars are SEM. At right, representative mEJC recordings, showing increased amplitude/frequency of mEJCs in *dfxrNOE* compared to wild-type, are shown.

(C) mEJC amplitude is slightly increased in both *dfxr* nulls (*dfxr*) and dFXR overexpression lines (MOE and NOE). At left, mean mEJC amplitude is slightly but significantly increased in all *dfxr* genotypes (one asterisk indicates $p < 0.05$, two asterisks indicates $p < 0.01$ by Mann-Whitney U test). Error bars are SEM. At right, amplitude distributions in all genotypes were similar.

Moreover, microtubules play an essential role in the transport and subsequent regulation of synaptic vesicle dynamics underlying neurotransmission (Rodesch and Brodie, 2000). Based on these lines of reasoning, we

performed immunoprecipitation and Western analyses to determine whether Futsch expression is regulated by dFXR.

We first tested for a physical interaction between

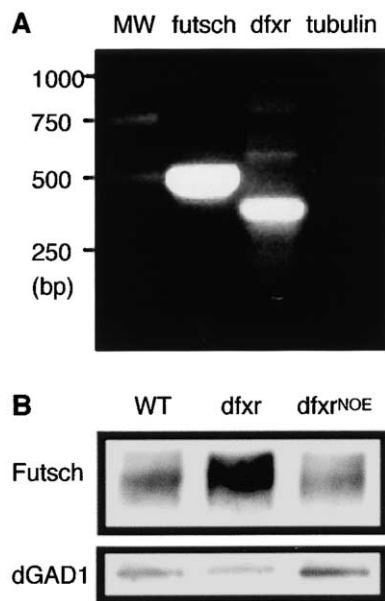


Figure 7. Futsch mRNA Is Associated with dFXR and Its Expression Negatively Regulated by dFXR

(A) *futsch* mRNA is present in dFXR-associated protein complex. Transcripts of *dfxr* and *futsch*, but not α -tubulin, are found in the protein complex immunoprecipitated by anti-dFXR. MW indicates molecular size shown in bp.

(B) Representative Western blot showing Futsch expression in wild-type (wt), *dfxr* nulls (*dfxr*), and *dfxr*^{NOE} mutants. The lower image shows dGAD1 antibody was used for loading control. The *dfxr* nulls show an elevated Futsch expression, whereas *dfxr*^{NOE} causes a significant reduction of Futsch expression.

dFXR protein and *futsch* mRNA (Figure 7A). We performed immunoprecipitation analyses using a monoclonal anti-dFXR to identify mRNAs that associate with the protein. First, as a positive control, RT-PCR showed that the protein complex immunoprecipitated by anti-dFXR contained *dfxr* mRNA, in agreement with previous findings with mammalian FMRP (Ashley et al., 1993a; Brown et al., 1998). Second, we showed that *futsch* mRNA was also present in the immunoprecipitated protein complex (Figure 7A). As a negative control, we showed that anti-dFXR immunoprecipitation did not pull down α -tubulin mRNA, which is highly expressed in brain. Subsequent sequencing of the RT-PCR products confirmed the association of dFXR and *futsch* mRNA. As a control for the immunoprecipitation specificity, the same treatments of *dfxr* null mutants produced no positive results (data not shown). These results demonstrate that dFXR protein specifically binds *futsch* mRNA and may regulate Futsch expression at a translational level.

Quantitative Western analyses showed that Futsch expression in the nervous system was inversely correlated with dFXR expression (Figure 7B). Initially, we observed alterations in the distribution and intensity of Futsch immunoreactivity in the nervous systems of *dfxr* mutants (data not shown). To quantify these changes in Futsch expression, we performed Western analyses on adult head extracts from *dfxr* mutants and *dfxr*^{NOE} lines. Futsch protein levels were significantly decreased to an average of $78.2\% \pm 2.5\%$ of control levels in *dfxr*^{NOE}

(Figure 7B). In *dfxr* null mutants, in contrast, Futsch was altered in the opposite direction, displaying an increase to $208\% \pm 32.4\%$ of control levels (Figure 7B). These results demonstrate that dFXR negatively regulates the expression of Futsch in the nervous system. The negative regulation of Futsch by dFXR, together with the binding of dFXR with *futsch* mRNA (Figure 7A) as well as previous reports of a role of FMRP in translational regulation, suggests that dFXR acts as a negative translational regulator of Futsch.

Futsch and dFXR Interact to Regulate Synaptic Structure and Function

Futsch regulates microtubules at the *Drosophila* NMJ (Roos et al., 2000). Therefore, we hypothesized that dFXR-dependent Futsch regulation might mediate the control of synaptic structure and function, explaining the synaptic dysfunction observed in *dfxr* mutants. Since *dfxr* null mutants elevate Futsch expression (Figure 7B), this model predicts that Futsch overexpression should mimic *dfxr* synaptic phenotypes. Similarly, dFXR overexpression decreases Futsch expression (Figure 7B), so *futsch* hypomorph mutants should display *dfxr*^{NOE} phenotypes. Finally, double mutants of *dfxr futsch* would be predicted to rescue *dfxr* synaptic structure and function phenotypes. We tested these predictions in *futsch* mutants, *futsch* transgenic NOE lines, and *dfxr futsch* double mutants by assaying synaptic structure and neurotransmission at both the larval NMJ and adult eye.

Consistent with the hypothesis, *futsch*^{NOE} caused an NMJ overgrowth phenotype similar to *dfxr* null mutants, with increased synaptic area, branching, and bouton number (Figure 8A; Roos et al., 2000). Also consistent with the hypothesis, hypomorphic *futsch* mutants display reduced NMJ growth and enlarged synaptic boutons (Roos et al., 2000), similar to *dfxr*^{NOE} (Figure 8B). Therefore, we made a *dfxr futsch* double mutant (*dfxr* null allele 50M; *futsch* hypomorph allele N94) and assayed NMJ structure. The double mutant forms a structurally normal NMJ indistinguishable from control (wt) in regards to synaptic branching and bouton number (Figure 8A: 3.95 ± 0.38 branches in wt versus 4.1 ± 0.48 in double mutant; 41.52 ± 1.85 boutons in wt versus 41 ± 2.05 in double mutant). These results demonstrate that upregulation of Futsch is sufficient to explain the synaptic structural defects caused by dFXR loss-of-function.

We next performed functional assays of neurotransmission in the eye and NMJ with *futsch* hypomorphs and NOE lines to determine whether the regulation fits predictions from the model. Consistent with the hypothesis, both *futsch* hypomorphs and *futsch*^{NOE} elevated neurotransmission at the NMJ (Figure 8C; *futsch*^{NOE} 46.22 nA versus 35 nA in wt). Also consistent with the hypothesis, both *futsch* hypomorphs and *futsch*^{NOE} significantly reduced photoreceptor neurotransmission (Figure 8D; *futsch*^{NOE} 3.47 mV versus 7.19 mV in wt). It is particularly striking that either loss or overexpression of both *dfxr* and *futsch* had identical effects on synaptic transmission, i.e., elevated at the NMJ and suppressed in the eye.

These observations suggest that precise regulation of Futsch levels by dFXR is required to properly maintain transmission in central and peripheral synapses. If the

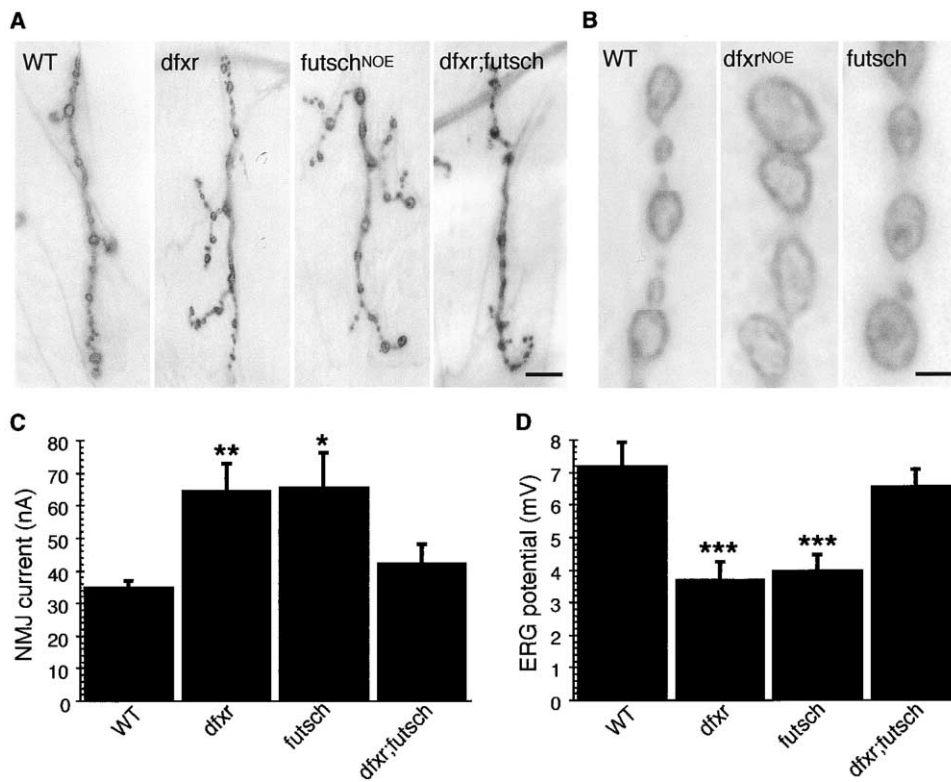


Figure 8. Synaptic Phenotypes of *dfxr* Nulls Are Suppressed by *futsch* Mutants

(A) *dfxr* null (*dfxr*) and Futsch overexpression (*futsch*^{NOE}) had similar phenotypes of NMJ terminal overgrowth, increased arboreal branching, and increased number of synaptic boutons. Double mutants of *dfxr futsch* suppressed the overgrown phenotype. The scale bar equals 10 μ M. (B) Both *dfxr* NOE (*dfxr*^{NOE}) and *futsch* hypomorph (*futsch*) showed fewer but larger synaptic boutons. The scale bar equals 2 μ M. (C) Double mutants of *dfxr futsch* restore the NMJ-evoked neurotransmissions to wild-type level (one asterisks indicates $p < 0.05$, two asterisks indicate $p < 0.01$; $n \geq 8$). (D) Double mutants of *dfxr futsch* restore the photoreceptor synaptic transmissions shown by ERG to wild-type level (three asterisks indicate $p < 0.001$; $n \geq 5$).

defects observed in *dfxr* mutants are due to the upregulation of Futsch levels, then one should be able to bring the levels of Futsch down to compensate by combining *dfxr* nulls with *futsch* hypomorphs in the same genome. We generated the double mutants of *dfxr futsch* and assayed synaptic transmission at the NMJ and in the eye. We observed a remarkable suppression of synaptic defects observed in *dfxr* mutants (Figures 8C and 8D). In the NMJ, the double mutant reduced transmission to levels indistinguishable from controls (Figure 8C), whereas in the eye, the double mutant increased neurotransmission to wild-type levels (Figure 8D). This genetic suppression provides convincing evidence that dFXR regulates synaptic mechanisms entirely through its regulation of Futsch. Taken together, this study strongly supports the hypothesis that dFXR acts as a translational repressor of Futsch to regulate microtubule dynamics and thereby control synaptic structure and function.

Discussion

The *Drosophila* Genome Encodes a Single, Conserved Member of the FMRP Family

Although early attempts to identify a *Drosophila* homolog of *FMR1* yielded no positive results (Verkerk et al.,

1991; Siomi et al., 1993), it is now clear that *Drosophila* contains a single, functionally conserved member of the *FMR1* family, *dfxr* (Wan et al., 2000 and this work), compared to the three related genes present in mammals. The molecular characteristics, cellular and subcellular expression pattern, and functions of *Drosophila* FXR and mammalian FMRP show extensive parallels. Most importantly, *dfxr* mutant phenotypes are consistent with the synaptic defects associated with human FraX patients and *FMR1* knockout mice. These observations suggest *Drosophila* is an attractive genetic system to model FraX.

At a gross level, lack of *Drosophila* FXR and mammalian FMRP have similar consequences. In both cases the gene is not essential; null mutants are adult viable with a normal developmental time course. Behaviorally, both *Drosophila* and mammalian mutants show locomotor deficits. Although we cannot draw a direct comparison between flight defects in the *dfxr* mutants and movement abnormalities in FraX patients, it is interesting to note that both display impaired motor control. FraX patients have visuospatial defects and *Drosophila dfxr* mutants show decreased photoreceptor function in the retina. All of these common defects can be readily explained by impaired synaptic development or function.

dFXR Plays Structural and Functional Roles at Synapses

Recent studies indicate that mammalian FMRP is present at synapses and regulates synaptic structure (Comery et al., 1997; Feng et al., 1997b; Tamanini et al., 1997; Weiler et al., 1997; Nimchinsky et al., 2001). Similarly, *Drosophila* dFXR is highly expressed in both pre- and postsynaptic neurons, as well as in postsynaptic muscles (Figure 2), and regulates synaptic structure (Figure 5). Overgrowth of dendritic spines, sites of synaptic input, is a diagnostic characteristic in FraX patients (Hinton et al., 1991; Irwin et al., 2001) and also is the primary phenotype of *FMR1* knockout mice (Comery et al. 1997; Nimchinsky et al., 2001), suggesting a common synaptic basis of the disease. Similarly in the *dfxr* null, NMJ synaptic terminals are overgrown, containing more arboreal branches and more synaptic boutons. We do not presently know whether human patients and *FMR1* knockout mice show similar NMJ defects. In addition, we found that dFXR overexpression had the opposite and complementary consequence of inhibiting synaptic growth and arborization. Thus, synaptic growth, branching, and bouton differentiation are negatively regulated proportional to dFXR levels.

dFXR is also a key regulator of synaptic function. We show that different functional/chemical classes of synapses respond differently to dFXR misregulation. In the eye, histaminergic photoreceptor neurotransmission is equally impaired by either loss or overexpression of dFXR, demonstrating that a precise level of the protein is required to maintain synaptic function. At the peripheral glutamateric NMJ, in contrast, neurotransmission is strikingly enhanced by either loss or overexpression of dFXR. The role of dFXR is primarily presynaptic, mediating synaptic vesicle fusion probability. We currently do not know why the polarity of dFXR regulation differs between these central and peripheral synapses.

Taken together, these results strongly support a dFXR/FMRP synaptic function: dFXR and FMRP are similarly expressed in pre/postsynaptic cells, play a conserved role in dendritic spine/synapse structural regulation, and dFXR, at least, is required for differential regulation of synaptic neurotransmission. We suggest that the FMRP family plays a conserved role in synaptic development and function, which likely underlies the behavioral and developmental symptoms of FraX patients.

dFXR Negatively Regulates the Expression of Futsch, a Homolog of Microtubule-Associated MAP1B

The expression of FMRP is increased locally following glutamate receptor stimulation, suggesting that FMRP acts as a synaptic activity-dependent translational regulator (Weiler et al., 1997; Jin and Warren, 2000). Recent evidence has shown that FMRP is a negative translational regulator (Laggerbauer et al., 2001; Li et al., 2001; Schaeffer et al., 2001). Given these studies, we hypothesized that dFXR may act as a translational repressor mediating the coupled regulation of synaptic structure and function. Several lines of evidence suggested that Futsch, a microtubule-associated MAP1B homolog, may be a target for dFXR translational regulation in the *Drosophila* nervous system. Futsch is required for den-

dritic and axonal development, as well as for synaptic growth (Hummel et al., 2000; Roos et al., 2000). Moreover, *futsch* mutants alter *Drosophila* NMJ architecture in a fashion similar to *dfxr* NOE animals. Misregulation of the microtubule-based synaptic cytoskeleton appeared a likely candidate for the coupled structural and functional defects observed in *dfxr* mutants.

We provide evidence that dFXR negatively regulates Futsch expression. First, dFXR associates with *futsch* mRNA (Figure 7A). This interaction is specific, since dFXR fails to bind other targets such as α -tubulin mRNAs and the interaction is missing in *dfxr* null mutants. Second, in *dfxr* null mutants, Futsch protein level in the nervous system is increased and dFXR neuronal overexpression causes Futsch expression to be reduced. These results show that the level of Futsch in the nervous system is inversely regulated by the level of dFXR. Taken together, the biochemical association between dFXR protein and *futsch* mRNA and the inverse regulation of Futsch expression by dFXR strongly support a hypothesis that dFXR acts as a negative regulator of Futsch translation.

Futsch appears to be the major target for dFXR in the regulation of synaptic structure and function. Structurally, *futsch* hypomorphs displayed fewer and enlarged NMJ synaptic boutons with dispersed, punctate anti-Futsch immunoreactivity, a phenotype indistinguishable from that caused by *dfxr*^{NOE}. Contrariwise, *futsch*^{NOE} caused synaptic overgrowth, a phenotype similar to *dfxr* null mutants. Functionally, all four genotypes (loss and overexpression of either dFXR or Futsch) enhanced neurotransmission at the larval NMJ, and all four genotypes impaired neurotransmission in the adult eye. Thus, the expression alterations of Futsch are sufficient to explain the synaptic phenotypes of *dfxr* mutants.

The most conclusive experimental result is the suppression of *dfxr* synaptic phenotypes by the *dfxr futsch* double mutants (Figure 8). The double mutant develops normal synaptic architecture, including the normal number of arboreal branches and synaptic boutons. Strikingly, the double mutant reduces NMJ transmission to suppress the peripheral synaptic phenotype, while at the same time it increases photoreceptor transmission to suppress the central synaptic phenotype. Based on these results, we propose that the major function of dFXR is the negative regulation of Futsch in the nervous system, which in turn regulates microtubule-dependent synaptic structure and function. Of course, it remains probable that dFXR is translationally regulating multiple proteins. However, we stress that the Futsch misregulation is sufficient to explain the synaptic phenotypes in *dfxr* mutants and, by extrapolation, possibly the mental retardation of FraX patients.

Experimental Procedures

Molecular Techniques

The Berkeley *Drosophila* Genome Project (BDGP) EST database (<http://www.fruitfly.org>) was searched against a human FMRP sequence (GenBank accession number S65791). Two overlapping EST clones (LD09557 and GH26194) with high homology to the FMRP NH2 terminal were obtained and sequenced. P1 clone DS05441 was obtained from BDGP, and the corresponding *dfxr* genomic region was sequenced. To characterize *dfxr* deletions, excision lines were

screened by PCR using the GeneAmp kit (Perkin Elmer) with primers 48 (aaggaaaaagcggccgcaaatatcgcgaaatccccccag) and 57 (cgggatccggttgctacgtgaataa). For overexpression studies, a UAS-dFXR construct was made by introducing the entire LD09557 cDNA insert into the transformation vector pUAST. Site-specific mutagenesis to generate the I307N mutation was performed with the ExSite kit (Stratagene) and primer 37 (gtccacaatctcgtgtaatgcccattctgccc).

Immunoprecipitation and RNA Identification by RT-PCR

Protein A beads (Pierce) were washed four times with PBST. dFXR antibody (22 μ l) (Wan et al., 2000) was diluted to 500 μ l with PBST and incubated with the protein A beads for 1 hr at RT followed by coupling with disuccinimidyl suberate. Beads were then washed four times with PBS + 0.2 M glycine, once with 1 M NaCl, and equilibrated with lysis buffer (in mM): 50 Tris (pH 7.2), 150 KCl, 1 EGTA, and 0.5% TX 100. Fly heads were isolated by agitation and subsequent sieving after freezing in liquid N₂. Heads (0.3–0.5 g) were homogenized in lysis buffer with a Dounce homogenizer, followed by centrifugation for 10 min at 6000 \times g. The pretreated beads and head extract were mixed and incubated for 1 hr at 4°C, followed by washing five times with lysis buffer. The bound RNA transcripts were eluted with lysis buffer plus 1 M NaCl. Elutions were pooled and precipitated with glycogen and ethanol. First-strand synthesis was achieved with Superscript II. This product (2 μ l) was used in a 100 μ l PCR reaction with Taq polymerase using gene specific primers spanning at least one intron.

Genetics

Drosophila stocks were cultured on standard medium. All marker mutations are as described in Lindsley and Zimm (1992). EP(3)3517 and EP(3)3422 from BDGP were outcrossed to wild-type flies to clean up genetic backgrounds. Excision derivatives of EP(3)3517 were generated by introducing $\Delta 2-3$ into the genome following standard procedures. Deficiency *Df(3R)by62* (chromosomal fragment from 85D11-13 to 85F16 including *dfxr* deleted) was obtained from the Bloomington *Drosophila* Stock Center. Mutant larvae or adults over *Df(3R)by62* were selected for all phenotypic analyses. *Drosophila* strain OR was used as wild-type control. Futsch hypomorph allele N94 (Roos et al., 2000) was used for double-mutant assays. UAS transgenic lines were generated by coinjection of the UAS construct with a $\Delta 2-3$ helper plasmid into *w¹¹¹⁸* embryos following standard protocols. For overexpression studies, the GAL4-UAS transgenic system (Brand and Perrimon, 1993) was used. To cooverexpress wild-type and mutant I307N dFXR, UAS-dFXR and UAS-I307N were recombined on the same chromosome using standard genetic methods. GAL4 lines used in this work were eye-specific sev-GAL4 from B. Dickson, nervous system-specific elav-GAL4, and muscle-specific GAL4 line *mhc-GAL4* from C. Goodman. An independent muscle expression line G7-GAL4 was isolated by C. Rodesh.

Flight Test

The flight test was done according to a protocol designed by Benzer (1973). Briefly, a 1000 ml graduated cylinder was used, and the inside wall was coated with mineral oil. Flies (1–2 days after eclosion) were placed into the top of the cylinder through a funnel to initiate flight (Figure 3C). The height flies stick in the cylinder reflects their flight ability. To test flight ability individually, a single fly was released from a small vial by opening the lid and tapping the vial. Flight was scored based on the percentage to initiate flight relative to flightless animals.

Immunocytological Staining and Western Analyses

Preparation and antibody staining for whole-mount embryos and dissected third instar larvae have been described elsewhere (Broadie and Bate, 1993; Beumer et al., 1999). Whole-mount adult brains were prepared as follows: following proboscis removal, the head was fixed in 4% formaldehyde for 30 min, and then the brain was dissected free and fixed for another 30 min. The following antibodies were used: monoclonal anti-dFXR (1:1000) from Dr. G. Dreyfuss (Wan et al., 2000); rabbit anti-synaptotagmin (1:500) from H. Bellen; rabbit anti-discs-large (1:1000) from D. Woods; monoclonal anti-cysteine string protein (1:500) from K. Zinsmaier; and monoclonal

anti-22C10 against Futsch (1:100) from Developmental Studies Hybridoma Bank, University of Iowa. Anti-mouse and anti-rabbit secondary antibodies conjugated to fluorescent tag (Molecular Probes) or horseradish peroxidase (Amersham) were used at 1:100. Propidium iodide (1.25 μ g/ml) for nuclear staining was applied for 20 min at RT. Serial sections of antibody or dye stained preparations were acquired on a Bio-Rad MRC 600 laser-scanning confocal microscope with LaserSharp2000 software.

Quantification of NMJ morphological features was done as described (Beumer et al., 1999; Rohrbough et al., 2000). For bouton size, type 1b terminals from muscle 6/7 were analyzed following Roos et al. (2000). Quantitative Western analyses were done as described (Fergestad et al., 1999). Briefly, adult *Drosophila* heads were homogenized in lysis buffer (50 mM Tris [pH 7.5], 150 mM NaCl, 1% NP-40, and 1 \times complete protease inhibitor [Boehringer Mannheim]) and subjected to SDS-PAGE electrophoresis on a 4%–20% gradient Tris-HCl gel (Bio-Rad). For the loading control, an antibody against *Drosophila* glutamate decarboxylase 1 antibody (dGAD1, provided by Dr. Rob Jackson) was used at 1:1000.

Electrophysiology: Two Electrode Voltage Clamp (TEVC) and Electoretinogram (ERG)

TEVC recordings were performed on muscle 6 in the abdominal segments 2/3 of the third instar as described (Rohrbough et al., 2000). Briefly, recordings were made at 18°C with sharp glass electrodes filled with 3:1 mixture of 3 M KAc/KCl. Nerve stimulation was achieved by a brief (0.5–0.8 ms at 0.5 Hz) positive current via a suction electrode. Recording bath solution was a modified standard saline, consisting of (in mM) 128 NaCl, 2 KCl, 4 MgCl₂, 70 sucrose, 5 HEPES (pH 7.2), and 0.4 CaCl₂. A total of 40 responses were recorded per larva and averaged to give each datum. Miniature excitatory junctional currents (mEJC) were assayed in 0.2 mM Ca²⁺ modified standard saline with 2.5–5 μ M tetrodotoxin (TTX, Sigma Chemicals) to block endogenous activity.

ERG recordings were performed as described (Broadie, 2000). Briefly, specimens were anesthetized with CO₂ and embedded in dental wax. The recording protocol was as follows: dark-adapted for 5 min, 1 s light recording followed by 9 s of dark. This was repeated four times without pause, with the five traces averaged to give each datum. Data points were collected at the initiation and the peak of the off transient. The magnitude of the off transient is the absolute difference in millivolts between the two points.

GenBank Accession Number

For the two *dfxr* cDNA sequences, the GenBank accession numbers are AF205596 and AJ271221; for the genomic sequence, the accession number is AF205597.

Acknowledgments

We are indebted to the Berkeley *Drosophila* Genome Project for EP lines and clones. We are particular grateful to G. Dreyfuss for his gift of dFXR antibody. We thank G. Davis for *futsch* alleles; K. Zinsmaier, T. Littleton, D. Woods, and R. Jackson for anti-CSP, anti-syt, anti-DLG, and anti-dGAD1, respectively; B. Dickson for sev-GAL4; M. Bastiani for access to confocal imaging; S. Mullaney for germline transformation services; and J. Rehm for inverse PCR data. M. Evans, C. Suh, G. Tsang, and A. Wong participated in DNA sequencing. Y.Q.Z. was supported by a fellowship from the FRAXA Research Foundation. A.M.B. was a fellow of the Helen Hay Whitney Foundation. R.B.R. was supported by a National Institutes of Health training grant ST32 HD07491. G.M.R. is an Investigator of the Howard Hughes Medical Institute. K.B. is supported by an EJLB Scholarship and by National Institutes of Health grant HD40654.

Received June 22, 2001; revised November 5, 2001.

References

Ashley, C.T., Jr., Wilkinson, K.D., Reines, D., and Warren, S.T. (1993a). FMR1 protein: conserved RNP family domains and selective RNA binding. *Science* 262, 563–566.

- Ashley, C.T., Jr., Sutcliffe, J.S., Kunst, C.B., Leiner, H.A., Eichler, E.E., Nelson, D.L., and Warren, S.T. (1993b). Human and murine FMR-1: alternative splicing and translational initiation downstream of the CGG-repeat. *Nat. Genet.* **4**, 244–251.
- Benzer, S. (1973). Genetic dissection of behavior. *Sci. Am.* **229**, 24–37.
- Beumer, K.J., Rohrbough, J., Prokop, A., and Broadie, K. (1999). A role for PS integrins in morphological growth and synaptic function at the postembryonic neuromuscular junction of *Drosophila*. *Development* **126**, 5833–5846.
- Brand, A.H., and Perrimon, N. (1993). Targeted gene expression as a means of altering cell fates and generating dominant phenotypes. *Development* **118**, 401–415.
- Broadie, K.S. (2000). Functional assays of the peripheral and central nervous system. In *Drosophila* Protocols, W. Sullivan, M. Ashburner, and R. S. Hawley, eds. (Cold Spring Harbor, New York: Cold Spring Harbor Laboratory Press), pp. 297–311.
- Broadie, K.S., and Bate, M. (1993). Development of the embryonic neuromuscular synapse of *Drosophila melanogaster*. *J. Neurosci.* **13**, 144–166.
- Brown, V., Small, K., Lakkis, L., Feng, Y., Gunter, C., Wilkinson, K.D., and Warren, S.T. (1998). Purified recombinant Fmrp exhibits selective RNA binding as an intrinsic property of the fragile X mental retardation protein. *J. Biol. Chem.* **273**, 15521–15527.
- Comery, T.A., Harris, J.B., Willems, P.J., Oostra, B.A., Irwin, S.A., Weiler, I.J., and Greenough, W.T. (1997). Abnormal dendritic spines in fragile X knockout mice: maturation and pruning deficits. *Proc. Natl. Acad. Sci. USA* **94**, 5401–5404.
- Devys, D., Lutz, Y., Rouyer, N., Bellocq, J.P., and Mandel, J.L. (1993). The FMR-1 protein is cytoplasmic, most abundant in neurons and appears normal in carriers of a fragile X premutation. *Nat. Genet.* **4**, 335–340.
- Eberhart, D.E., Malter, H.E., Feng, Y., and Warren, S.T. (1996). The fragile X mental retardation protein is a ribonucleoprotein containing both nuclear localization and nuclear export signals. *Hum. Mol. Genet.* **5**, 1083–1091.
- Feng, Y., Absher, D., Eberhart, D.E., Brown, V., Malter, H.E., and Warren, S.T. (1997a). FMRP associates with polyribosomes as an mRNP, and the I304N mutation of severe fragile X syndrome abolishes this association. *Mol. Cell* **7**, 109–118.
- Feng, Y., Gutekunst, C.A., Eberhart, D.E., Yi, H., Warren, S.T., and Hersch, S.M. (1997b). Fragile X mental retardation protein: nucleocytoplasmic shuttling and association with somatodendritic ribosomes. *J. Neurosci.* **17**, 1539–1547.
- Fergestad, T., Davis, W.S., and Broadie, K. (1999). The stoned proteins regulate synaptic vesicle recycling in the presynaptic terminal. *J. Neurosci.* **19**, 5847–5860.
- Hinton, V.J., Brown, W.T., Wisniewski, K., and Rudelli, R.D. (1991). Analysis of neocortex in three males with the fragile X syndrome. *Am. J. Med. Genet.* **41**, 289–294.
- Hummel, T., Krukkert, K., Roos, J., Davis, G., and Klambt, C. (2000). *Drosophila* Futsch/22C10 is a MAP1B-like protein required for dendritic and axonal development. *Neuron* **26**, 357–370.
- Ilius, M., Wolf, R., and Heisenberg, M. (1994). The central complex of *Drosophila melanogaster* is involved in flight control: studies on mutants and mosaics of the gene ellipsoid body open. *J. Neurogenet.* **9**, 189–206.
- Irwin, S.A., Patel, B., Idupulapati, M., Harris, J.B., Crisostomo, R.A., Larsen, B.P., Kooy, F., Willems, P.J., Cras, P., Kozlowski, P.B., et al. (2001). Abnormal dendritic spine characteristics in the temporal and visual cortices of patients with fragile-X syndrome: a quantitative examination. *Am. J. Med. Genet.* **98**, 161–167.
- Jin, P., and Warren, S.T. (2000). Understanding the molecular basis of fragile X syndrome. *Hum. Mol. Genet.* **9**, 901–908.
- Khandjian, E.W., Corbin, F., Woerly, S., and Rousseau, F. (1996). The fragile X mental retardation protein is associated with ribosomes. *Nat. Genet.* **12**, 91–93.
- Laggerbauer, B., Ostareck, D., Keidel, E.M., Ostareck-Lederer, A., and Fischer, U. (2001). Evidence that fragile X mental retardation protein is a negative regulator of translation. *Hum. Mol. Genet.* **10**, 329–338.
- Li, Z., Zhang, Y., Ku, L., Wilkinson, K.D., Warren, S.T., and Feng, Y. (2001). The fragile X mental retardation protein inhibits translation via interacting with mRNA. *Nucleic Acids Res.* **29**, 2276–2283.
- Lindsley, D.L., and Zimm, G.G. (1992). *The Genome of Drosophila melanogaster* (San Diego, California: Academic Press).
- Nimchinsky, E.A., Oberlander, A.M., and Svoboda, K. (2001). Abnormal development of dendritic spines in FMR1 knock-out mice. *J. Neurosci.* **21**, 5139–5146.
- Peier, A.M., McIlwain, K.L., Kenneson, A., Warren, S.T., Paylor, R., and Nelson, D.L. (2000). (Over)correction of FMR1 deficiency with YAC transgenics: behavioral and physical features. *Hum. Mol. Genet.* **9**, 1145–1159.
- Rodesch, C.K., and Broadie, K. (2000). Genetic studies in *Drosophila*: vesicle pools and cytoskeleton-based regulation of synaptic transmission. *Neuroreport* **11**, R45–53.
- Rohrbough, J., Grotewiel, M.S., Davis, R.L., and Broadie, K. (2000). Integrin-mediated regulation of synaptic morphology, transmission, and plasticity. *J. Neurosci.* **20**, 6868–6878.
- Roos, J., Hummel, T., Ng, N., Klambt, C., and Davis, G.W. (2000). *Drosophila* Futsch regulates synaptic microtubule organization and is necessary for synaptic growth. *Neuron* **26**, 371–382.
- Rorth, P., Szabo, K., Bailey, A., Laverty, T., Rehm, J., Rubin, G.M., Weigmann, K., Milan, M., Benes, V., Ansorge, W., and Cohen, S.M. (1998). Systematic gain-of-function genetics in *Drosophila*. *Development* **125**, 1049–1057.
- Schaeffer, C., Bardoni, B., Mandel, J.L., Ehresmann, B., Ehresmann, C., and Moine, H. (2001). The fragile X mental retardation protein binds specifically to its mRNA via a purine quartet motif. *EMBO J.* **20**, 4803–4813.
- Siomi, H., Siomi, M.C., Nussbaum, R.L., and Dreyfuss, G. (1993). The protein product of the fragile X gene, FMR1, has characteristics of an RNA-binding protein. *Cell* **74**, 291–298.
- Tamanini, F., Meijer, N., Verheij, C., Willems, P.J., Galjaard, H., Oostra, B.A., and Hoogeveen, A.T. (1996). FMRP is associated to the ribosomes via RNA. *Hum. Mol. Genet.* **5**, 809–813.
- Tamanini, F., Willemsen, R., van Unen, L., Bontekoe, C., Galjaard, H., Oostra, B.A., and Hoogeveen, A.T. (1997). Differential expression of FMR1, FXR1 and FXR2 proteins in human brain and testis. *Hum. Mol. Genet.* **6**, 1315–1322.
- Verheij, C., Bakker, C.E., de Graaff, E., Keulemans, J., Willemsen, R., Verkerk, A.J., Galjaard, H., Reuser, A.J., Hoogeveen, A.T., and Oostra, B.A. (1993). Characterization and localization of the FMR-1 gene product associated with fragile X syndrome. *Nature* **363**, 722–724.
- Verkerk, A.J., Pieretti, M., Sutcliffe, J.S., Fu, Y.H., Kuhl, D.P., Pizzuti, A., Reiner, O., Richards, S., Victoria, M.F., Zhang, F.P., et al. (1991). Identification of a gene (FMR-1) containing a CGG repeat coincident with a breakpoint cluster region exhibiting length variation in fragile X syndrome. *Cell* **65**, 905–914.
- Wan, L., Dockendorff, T.C., Jongens, T.A., and Dreyfuss, G. (2000). Characterization of dFMR1, a *Drosophila melanogaster* homolog of the fragile X mental retardation protein. *Mol. Cell. Biol.* **20**, 8536–8547.
- Weiler, I.J., Irwin, S.A., Klintsova, A.Y., Spencer, C.M., Brazelton, A.D., Miyashiro, K., Comery, T.A., Patel, B., Eberwine, J., and Greenough, W.T. (1997). Fragile X mental retardation protein is translated near synapses in response to neurotransmitter activation. *Proc. Natl. Acad. Sci. USA* **94**, 5395–5400.